Available online at www.sciencedirect.com
SCIENCE DIRECT®
Estuarine, Coastal and Shelf Science 56 (2003) 1141–1156
ESTUARINE COASTAL AND SHELF SCIENCE

Physical processes associated with high primary production in Saanich Inlet, British Columbia

A.E. Gargett*, D. Stucchi, F. Whitney

Institute of Ocean Sciences, Patricia Bay, P.O. Box 6000, Sidney, British Columbia, Canada V8L 4B2

Received 31 January 2002; received in revised form 3 June 2002; accepted 14 June 2002

Abstract

Saanich Inlet, British Columbia, has long been known for the presence, in most years, of anoxic bottom water. One factor contributing to this anoxia is a high level of primary production, which occurs as a major spring bloom followed by sporadic 'mini-blooms' throughout the summer and early fall. The process(es) by which new production is refueled after nutrient exhaustion caused by the spring bloom are not well known, since Saanich is an inverse estuary and vertical mixing driven by winds and tides is low. This study presents new observational evidence that strongly suggests that the dominant mechanism of nutrient resupply during the summer months is intermittent advective exchange, driven by pressure gradients set up by strong tidal mixing in passages outside Saanich Inlet itself. A simple box model is formulated to illustrate this mechanism. When driven by annual freshwater forcing and deepwater renewal functions characteristic of the region and measured tides for 1975, the model predicts resupply of nitrate during most of the periods observed in 1975 observations (Deep-Sea Res. 24 (1977) 775). This 'action-at-a distance' nutrient resupply mechanism, involving strong but localized turbulent mixing and subsequent distribution of the products of mixing over large-horizontal distances by pressure-gradient-driven flow, is likely important in other coastal regions where the estuarine circulation is weak.

Keywords: plankton production; turbulent exchange; nutrient cycles; box model; Saanich Inlet

1. Introduction

It has long been argued that primary production in Saanich Inlet is larger than that in typical BC coastal inlets, hence a major contributory factor to observed anoxia of bottom waters despite relatively regular deepwater renewal events (Anderson & Devol, 1973). Timothy and Soon (2001) recently reported direct C^{14}-uptake measurements of primary productivity contrasting Saanich Inlet with Jervis Inlet, a 'normal' fjord-type estuary with oxygenated deep waters. Their multi-year observations confirm that average annual primary productivity in Saanich is indeed larger (roughly twice) than that in Jervis. An outstanding question is how such large primary productivity can be supported in an inlet, which superficially might be expected to have rather low primary production.

In most fjord-type estuaries, a brackish surface-layer flows outward as part of a normal estuarine circulation forced by dominant freshwater input at the head of the estuary. In such cases, biological new production is fueled by nitrate supplied by turbulent entrainment and pressure-gradient-driven upwelling of the base of the brackish layer. However, Saanich Inlet is an inverse estuary, with freshwater supplied dominantly outside the inlet mouth: in winter by the near-field effect of the Cowichan River and in summer by the far-field effect of the massive freshet of the Fraser River (Fig. 1). Thus, mean surface-layer estuarine flow driven by freshwater forcing should be into, rather than out of, the inlet, hence associated with downwelling, not upwelling in the interior. In addition, because Saanich Inlet is not strongly forced by either winds or tides (Herlinveaux,

* Corresponding author. Center for Coastal Physical Oceanography, Old Dominion University, Crittenton Hall 768 West 52nd Street, Norfolk, VA 23508, USA.
E-mail address: gargett@ccpo.odu.edu (A.E. Gargett).

0272-7714/03/$ - see front matter © 2003 Elsevier Science B.V. All rights reserved.
doi:10.1016/S0272-7714(02)00319-0

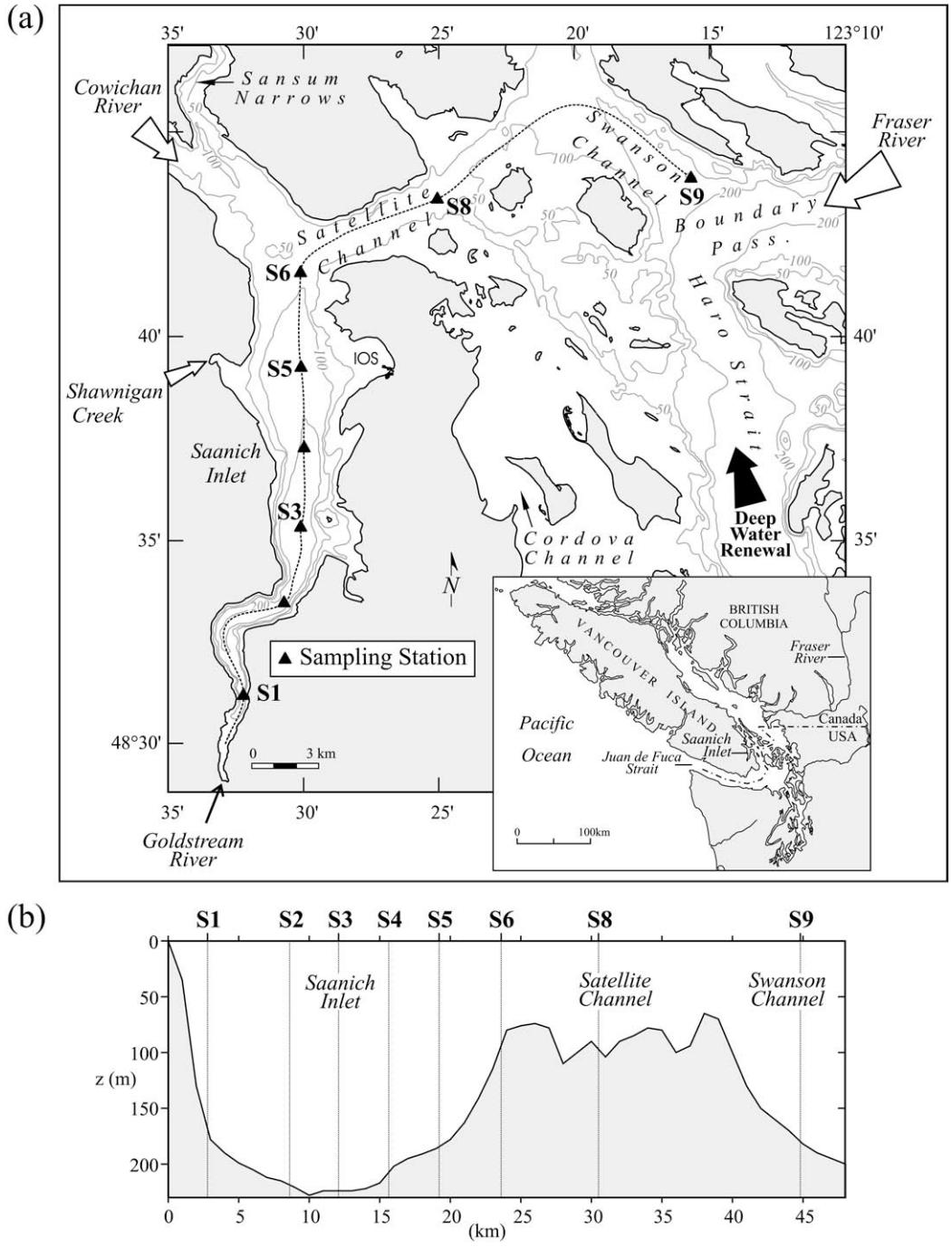

Fig. 1. (a) Location of sampling stations in Saanich Inlet, a fjord-type estuary on the southeastern tip of Vancouver Island, British Columbia (inset). Major sources of freshwater input are the nearby Cowichan River (winter) and the Fraser River (summer) on the mainland coast (inset), while deepwater renewal takes place through Haro Strait. (b) Vertical section, showing the deep inner basin of Saanich Inlet, and the extended sill region (Satellite Channel) connecting it to oceanic influence via Swanson Channel and Haro Strait.

1962), it has been assumed that the upper layers are characterized by low values of turbulent diffusivity. With inverse estuarine flow and low rates of turbulent nutrient resupply, high biological productivity in Saanich Inlet implies some other resupply process(es). Over time, the accumulation of various observations has suggested that possible mechanisms exist in the strong tidal mixing characteristic of regions just outside Saanich Inlet.

The first such evidence was provided by the documentation of Takahashi, Seibert, and Thomas (1977) on the detailed annual pattern of primary production of Saanich Inlet. Their study was the first to sample frequently enough (at least weekly) to describe not only the major

bloom, which occurs in spring and exhausts surface-layer nitrate, but also a characteristic succession of subsequent 'mini-blooms', which follow sporadic events of nitrate resupply during the summer and early fall. Noticing that increases in nitrate were correlated with increases in salinity (S), Takahashi et al. (1977) suggested that deeper, nutrient-rich waters were being moved nearer the surface by vertical mixing and/or vertical advection. Although no specific mechanism was suggested at the time, the time series observations of Takahashi et al. (1977, see their fig. 2) show a roughly fortnightly variability, suggesting some connection with the 14-day spring/neap tidal cycle. Indeed, Parsons, Perry, Nutbrown, Hsieh, and Lalli (1983) subsequently demonstrated significant anti-correlation between local tidal amplitude and the Takahashi et al. measurements of chlorophyll *a* at a period of 14 days. Parsons et al. (1983) went on to argue that the mouth of Saanich Inlet forms a frontal zone between stratified waters inside and strongly mixed (at least during spring tides) and nutrient-rich waters outside. The 14-day variability in primary production within Saanich could thus be driven by greater or lesser incursions of this front into the inlet as tidal velocities varied between spring and neap. This frontal mechanism almost surely contributes to the observed enhancement of primary production near the mouth relative to the head of Saanich Inlet (Timothy & Soon (2001) suggest a factor of 1.4 enhancement). However, because maximum frontal excursion cannot exceed the maximum tidal excursion (of order O(3 km)) in the vicinity of the mouth, this mechanism is unable to account for similar variation of nitrate resupply at stations near the head of Saanich Inlet (see Section 4, Fig. 7). Provided that primary production is reflected in export flux, the sediment trap measurements of Sancetta (1989) provide additional evidence that stations near the inlet head exhibit high frequency variability in primary production. This variability is probably associated with variable nitrate supply (keeping in mind that the 1-month sample interval of this study, considered normal (or even 'high frequency'!) for such coastal studies, significantly aliases a 14-day period). Thus, in addition to the localized resupply mechanism represented by frontal excursions near the mouth of Saanich Inlet, the observations require a mechanism which produces 'action-at-a-distance', i.e. a mechanism by which events outside Saanich can affect the entire inlet, not just areas nearest the mouth.

This purpose of this article is to present new observational evidence (Sections 3 and 4), which clarifies the physical mechanisms involved in this hypothesized 'action-at-a-distance'. While the suggested mechanism is physically quite different from that proposed by Parsons et al. (1983), the present study reinforces their general suggestion that tidally modulated variability in stratification outside Saanich Inlet is a major determinant of the oceanography and the biological productivity within it. In Section 5, a simple box model, forced by observed tides and simplified freshwater fluxes, is used to illustrate the salient processes by which new nutrient is supplied to fuel the high primary production of Saanich Inlet.

2. Physical characteristics of Saanich Inlet and environs

Saanich Inlet is a 24-km-long fjord-type inlet located at the southeastern end of Vancouver Island, British Columbia (Fig. 1a). While maximum depths exceed 200 m, a 75–80 m deep sill at the mouth of the inlet restricts the circulation of the deep basin waters (Fig. 1b). Unlike most Pacific fjords, the waters of the deep basin are devoid of dissolved oxygen—anoxic—for most of the year. Saanich Inlet is unusual in another respect, namely that physical processes and factors which force the circulation in most fjords are either absent or weak in this inlet.

Unlike normal estuaries, in which the major freshwater input occurs at the head of the inlet, there is relatively little freshwater discharge within Saanich Inlet itself because the catchment basin is rather small. The largest river flowing into the inlet (Shawnigan Creek, near the inlet mouth) has a maximum discharge of $O(4–5\,m^3\,s^{-1})$, predominantly in the winter rainy season. This local runoff is a minor percentage of two other sources of freshwater, both located outside the sill, which defines the mouth of Saanich Inlet. The Cowichan River, entering 10 km to the northwest (Fig. 1), has a winter maximum discharge of $O(20\,m^3\,s^{-1})$. Summer freshwater input to the region is dominated by the Fraser River, which discharges into the southern end of the Strait of Georgia within 50 km of the mouth of Saanich Inlet. Fraser River discharge contributes about half of the total freshwater supply to the Strait of Georgia (Griffin & LeBlond, 1990), which peaks in a June freshet fuelled by melting snow pack in the interior of the province. Maximum summer Fraser discharge of $O(8000\,m^3\,s^{-1})$ vastly exceeds that of even maximum (winter) values of the Cowichan, so that the Fraser River 'far-field' source dominates summertime freshwater forcing of Saanich Inlet. The freshet 'pulse' moves seaward from the southern Strait of Georgia to Juan de Fuca Strait and eventually out to the Pacific Ocean through a complex region of tidal channels among the Canadian Gulf Islands and the American San Juan Islands. Saanich Inlet is connected to Boundary Passage and Haro Strait, the major inter-island passages through this region, by Satellite and Swanson Channels (Fig. 1).

Both wind and tidal forcing of turbulence within Saanich Inlet are generally weak. Because the north/south axis of the inlet is roughly normal to prevailing winds, the wind field is much less energetic in Saanich than in most other BC inlets, which are oriented more nearly

east/west. There are no prominent diurnal sea breezes during the summer months, nor is the inlet subject to strong katabatic outflows of cold arctic air during winter months. Tidal currents are weak throughout Saanich Inlet. Moreover, since the sill is moderately deep and the mouth of the inlet is rather wide (3.5 km), the energetic interactions of a stratified flow with topographic constrictions (Farmer & Freeland, 1983) which are common in many other Pacific fjords, are not observed in this inlet. The weakness of wind and tidal forcings is consistent with available direct observations of turbulence properties. For several years, Saanich Inlet acted as a pre-cruise test site for micro-scale shear sampling, which provides profiles of turbulent kinetic energy dissipation rate ε, a commonly used metric for the strength of turbulent mixing (Tennekes & Lumley, 1972). As seen from the typical profiles of Fig. 2a, observed values of ε rarely rise above a system noise level of $O(10^{-9}\,m^2\,s^{-3})$, which translates, through standard micro-scale estimation (Gargett, 1997), to a diffusivity of $O(2\times10^{-6}\,m^2\,s^{-1})$. Using a mean nitrate gradient of $O(0.5\,mmol\,m^{-2} = 10(mmol\,m^{-3})/20\,m)$, typical of mid-inlet (see Fig. 6, Station S5), this diffusivity would produce a vertical nitrate flux of only $O(10^{-1}\,mmol\,m^{-2}day^{-1})$, much too small to account for measured fluxes of $O(4\,mmol\,m^{-2}day^{-1})$ during at least part of the fortnightly tidal cycle (see Section 4). Moreover, turbulent nitrate flux would be expected to be particularly weak during the summer months, due to a combination of weak winds and strong near-surface stratification caused by heating as well as freshening of the surface layer.

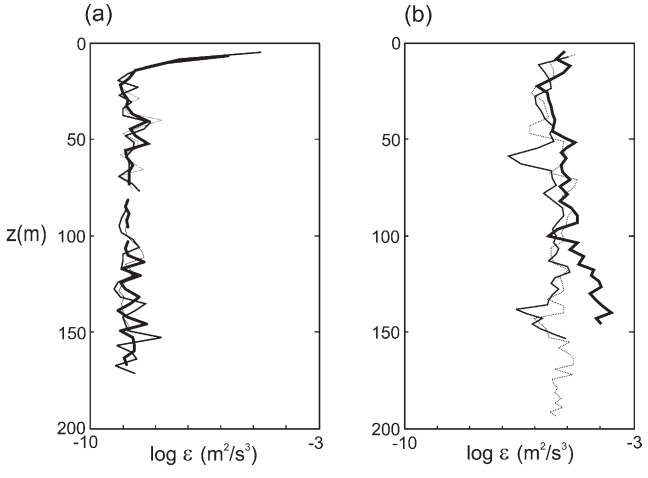

Fig. 2. Typical depth profiles of the logarithm of the turbulent kinetic energy dissipation rate ε, as determined from airfoil probes carried on a micro-scale profiler in (a) Saanich Inlet (Station S5) and (b) the Boundary Pass/Haro Strait tidal fronts that occur near the entrance (Station S9) to Swanson Channel, the major 'deepwater' pathway to Saanich Inlet. Assuming quasi-steady-state turbulence, the 3–4 orders of magnitude difference in ε between these two regimes implies similar difference in the rates at which energy is being supplied to turbulent motions.

While turbulence is weak within the inlet, it is anything but weak in many adjacent channels and passages. A large tidal volume, moving through contorted passages and over sills, produces strong (up to 4 kn) tidal currents that generate intense mixing in localized areas. Nearby locations (see Fig. 1), where strong mixing has been documented, include Sansum Narrows (Gargett, 1994), Cordova Channel (Lu & Lueck, 1999), and recurring tidal fronts (Farmer, D'Asaro, Trevorrow, & Dairiki, 1994; Gargett, 1994, 1999) in the region of Boundary Pass/Haro Strait near the mouth of Swanson Channel (see Fig. 1). As illustrated in Fig. 2b, turbulence in such areas can reach dissipation levels that are 3–4 orders of magnitude above the noise levels observed within Saanich. This tidally generated turbulence varies with the strength of tidal flows, hence is modulated at all significant tidal periods. At time scales longer than the dominant diurnal (K1) and semi-diurnal (M2) periods, tidal flows vary strongly with the fortnightly cycle that gives strongest flows during spring tides and weakest flows during neap tides. Measurements of ε made in Cordova Channel by Lu and Lueck (1999) provide direct evidence of an associated spring/neap cycle in tidal mixing. At longer periods, tidal mixing is expected to vary at the semi-annual period, which gives the strongest tidal flows of the year in June and December.

Because tidal mixing works against the stabilizing effect of seasonal freshwater input (and additional surface heating in the summer months), tidally driven variations in turbulence intensity result in large variations in density stratification in the region. Direct evidence of such variation is shown in Fig. 3. The color-coded background shows the evolution of the field of log ε (determined by an acoustic large-eddy method; Gargett, 1999) across a strong tidal front in Haro Strait over a 4-day period, as the tides increase from neap towards spring. Superimposed vertical profiles of density (σ_t) show that the late winter density structure, quasi-two-layer at the time of the neap tide, evolved into a much weaker, nearly linear stratification after only 4 days of increasing tidal flows and mixing. During maximum spring tides, water-column density may be nearly homogenized within such localized turbulent structures. Griffin and LeBlond (1990) provide indirect evidence that variation of turbulent mixing at the spring/neap periodicity strongly modulates seaward freshwater export in the upper layers of Juan de Fuca Strait.

3. Observational evidence of spring/neap tidal-forcing mechanism of mean flows

In July 1994, Canadian government agencies together with organizations of concerned citizens began the Saanich Inlet Study (SIS), a broadly based examination of the present state of the marine environment of the in-

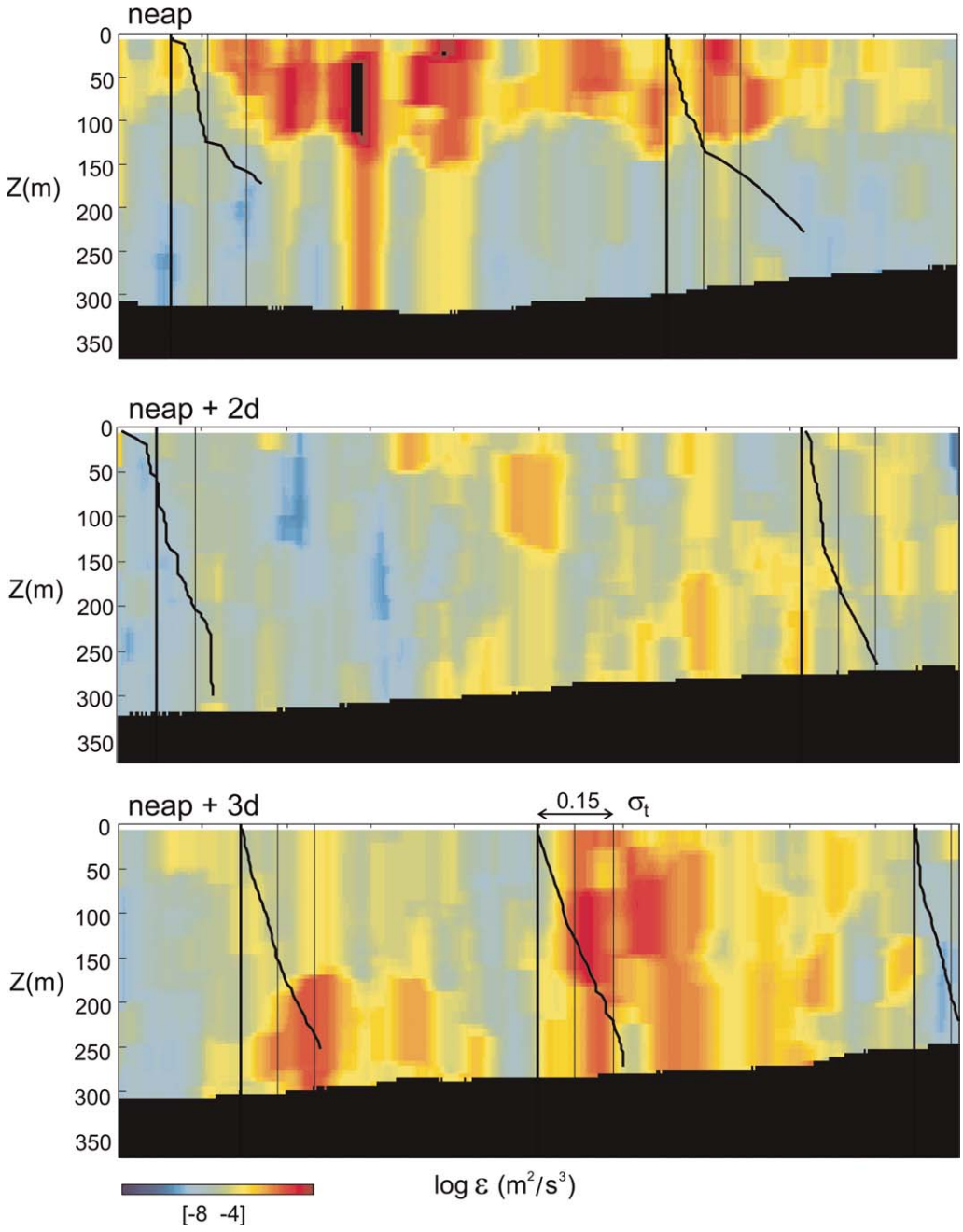

Fig. 3. Color codes the field of log ε, determined from a new acoustic large-eddy technique (Gargett, 1999), measured during approximately north/south (left to right) transects of a strong tidal front in Haro Strait as tides increased from neap towards spring. Superimposed vertical profiles of σ_t (courtesy of J. Moum, Oregon State University) show the effects of tidal mixing on the late winter density structure, quasi-two-layer at the beginning, but evolving quickly to a much weaker, nearly linear stratification after only 4 days of increasing tidal flows and turbulent mixing.

let and its ability to assimilate wastes from future development around its shores. During the SIS, a short-term measurement program was undertaken to address gaps in oceanographic data relating to circulation and nutrient transport above sill depth. The results presented in this study came from an intensive sampling period from July 5 to 20, 1995. Both shallow-drogued drifter tracks and water property variations measured during this period provide clear evidence of the dominant process that drives the shallow circulation.

Over the period July 10 to 20, sets of drifters drogued to follow the top 2 m of the water column were deployed and tracked. During the week of neap tides (Fig. 4a), drifters deployed in Finlayson Arm, the narrowest part of the inlet, exhibit the back and forth motion associated with the semi-diurnal tide, superimposed on a slight

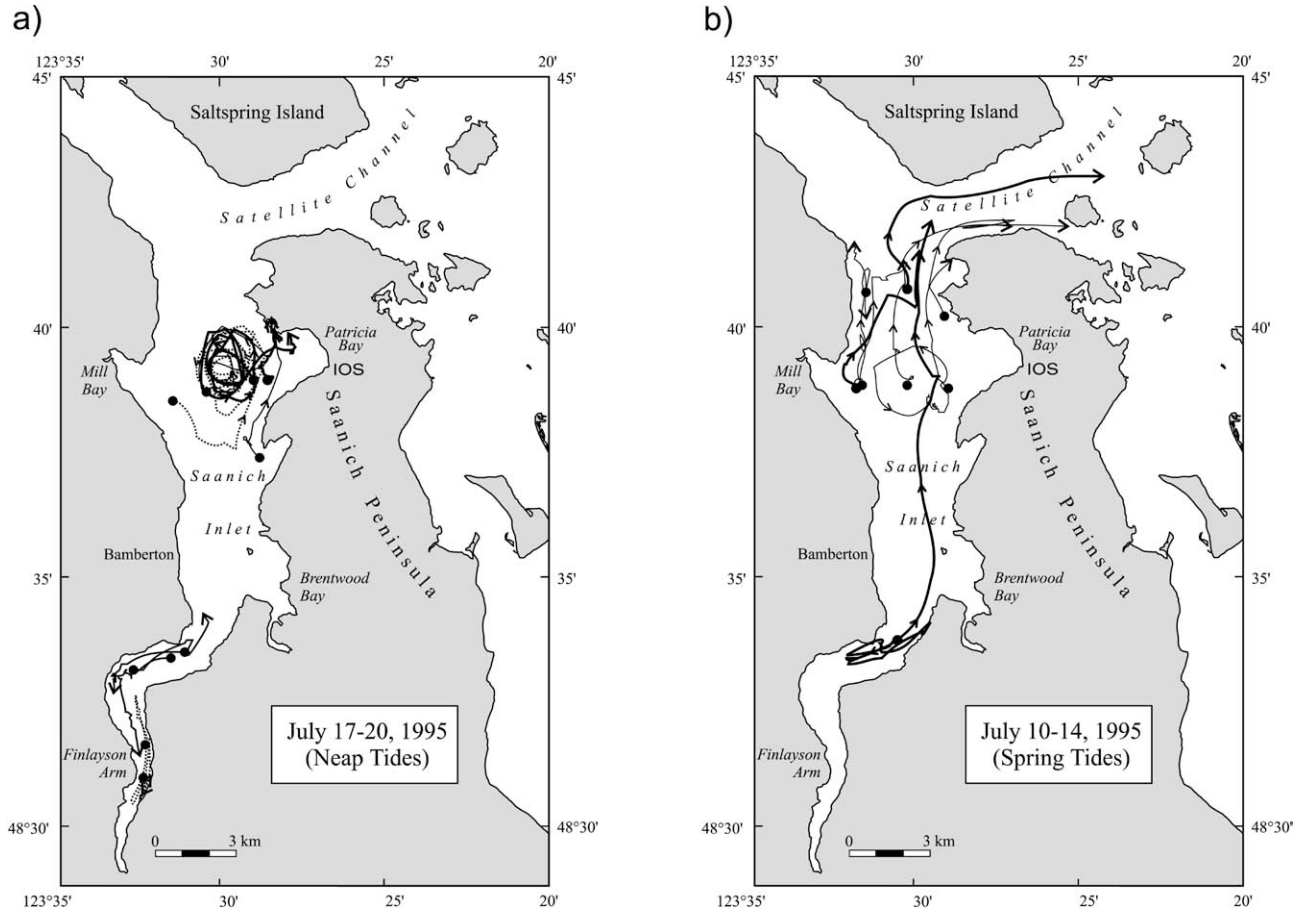

Fig. 4. Time histories of radio-tracked surface drifters, drogued at 2 m to reveal surface-layer motion, over 5-day intervals during (a) neap and (b) spring tides.

tendency for net up-inlet (southerly) movement. At the broader northern end of the inlet, most of the drifters appear locked in a CCW rotating 'eddy', associated with weak inflow(outflow) on the western(eastern) side of the inlet. No drifters left the inlet, although several grounded on the eastern shore.

In startling contrast (Fig. 4b), as tides built towards the spring tidal maximum, most of the drifters deployed in the northern part of the inlet moved swiftly northward and out of the inlet. Of the drifters deployed in the lower reaches of the inlet, most grounded immediately. However, one drifter set in Finlayson Arm moved back and forth for a couple of days and then proceeded northward covering the entire length of the inlet. During this period of time, winds were generally weak, hence could not be responsible for the observed northward transport of floats.

The combined drifter results suggest that spring/neap variation in tidal flows somehow produces strong modification of *non-tidal* horizontal flow, resulting in periodic reversals of the weak surface inflow, which characterizes an inverse estuary such as Saanich. Moreover, such reversals involve the entire inlet, not just the regions nearest the mouth. Reversal periods, during which Saanich Inlet temporarily behaves as a normal estuary, will be associated with a 'normal' estuarine upwelling/entrainment of nutrient-rich deep waters, which flow in at depth to compensate for the surface-layer outflow.

The mechanism involved in translating tidal variability into mean flows is suggested by salinity sections that were taken from the head of Saanich Inlet, out through the connecting passages (Satellite and Swanson Channels) to the major external deepwater channel (Haro Strait/Boundary Pass). Fig. 5a,c shows sections taken during two neap tides bracketing the spring tide section of Fig. 5b. The first neap tide survey (July 6) shows waters with $S < 29.0$ occupying the top 20 m of most of the inlet. One week later, at the time of spring tides, only a vestige of waters with $S < 29.0$ remained in the inlet. The layer of salinities between 29.0 and 30.0 had thickened within the inlet, as the 29.0 isohaline moved upward in the water column, and disappeared entirely outside the inlet. The following neap tide survey (July 20) shows that water with $S < 29.0$ had reoccupied the entire length of the inlet. Local runoff cannot account for the observed replenishment of the low salinity layer during the second neap tide period. Only 10.3 mm of rain fell in the area from the

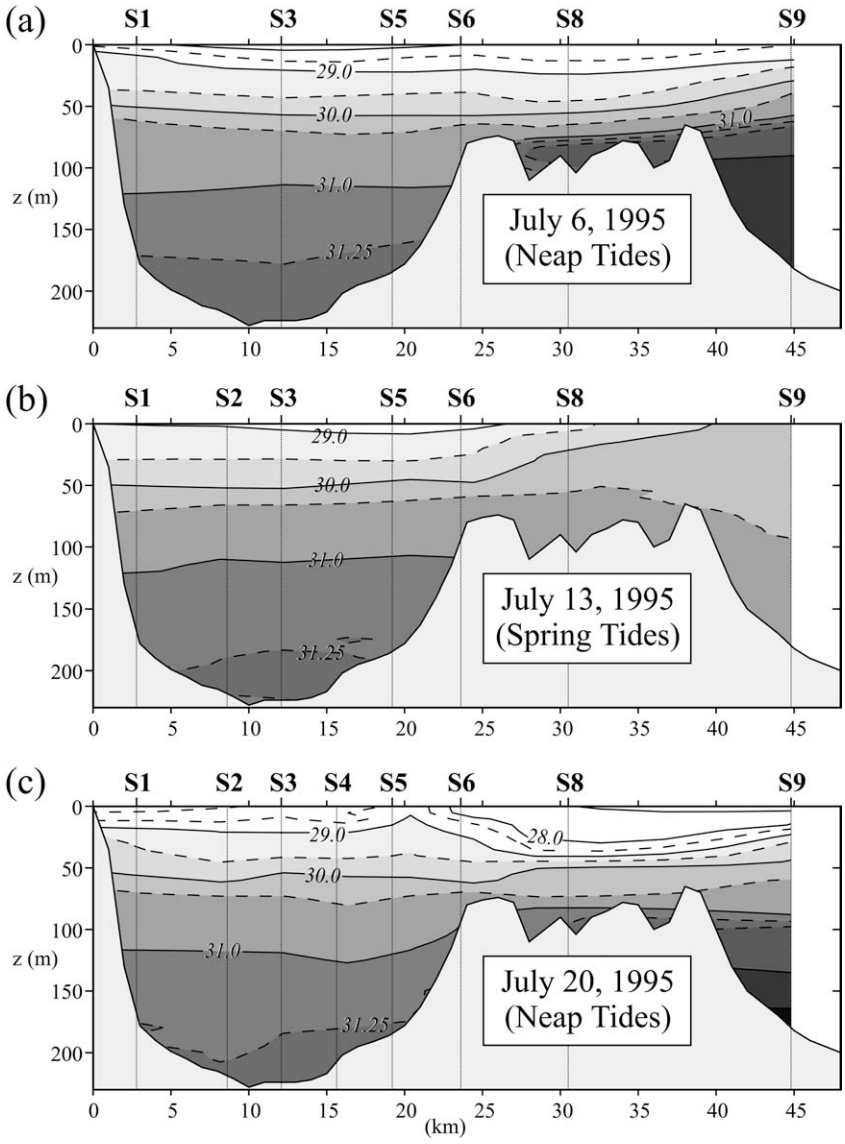

Fig. 5. Sections of salinity, S, taken from the head of Saanich Inlet (left) through the extended sill region outside its mouth and into deeper water near the junction of Swanson Channel and Haro Strait (right). Two sections taken during neap tides (a) July 6 and (c) July 20 are separated by a section taken during the intervening spring tide on (b) July 13. Note the virtual disappearance of low salinity water $S < 29.0$ from Saanich Inlet and the weakness of salinity stratification outside the inlet in the spring tide section.

last week in June to the last week in July, with most falling on July 9 and 10, just before the spring-tide flushing of low-salinity water from the inlet. In addition, other water properties unaffected by precipitation (temperature and dissolved oxygen, unpublished data) show similar large-scale changes during the three surveys.

Because density is determined predominantly by salinity in this area, there are major changes in stratification associated with the observed changes in the salinity field. While quantitative details differ, both neap tide sections reveal strong near-surface density stratification through the entire section. During the spring tides, there is a reduction of stratification within the inlet, but the largest changes are observed in the density gradients *outside* the inlet. Stratification is greatly reduced both in the shallow approaches (Satellite Channel) and the deeper connection (Swanson Channel) to Haro Strait (far right hand side of Fig. 5), where neap tide salinity differences of ~2.5–3.0 from surface to 100 m become differences of only ~0.5 at spring tides. In the face of continuing freshwater input from the Fraser River, the observed spring tide reduction in stratification in these areas external to Saanich Inlet can only result from increased tidal mixing, as documented in Section 3.

4. Time series of nitrogen species in Saanich Inlet

To this point, data and discussions have dealt with the physical circulation and water property changes

which occur inside Saanich Inlet in response to changing density and stratification outside. We now turn our attention to the effects of this variation in the physical system on transport and cycling of nitrogen and the biological productivity of this fjord.

Because nitrate supply periodically limits summer phytoplankton growth in Saanich Inlet (Takahashi et al., 1977), it is necessary to understand the mechanisms by which nutrients are resupplied to the euphotic zone before we can describe plankton dynamics over the entire summer growth season. Consequently, the SIS included a sampling program aimed at resolving the transport of nitrogen in its biologically active forms over the spring/neap cycle. Three stations (S3, S5 and S6, see Fig. 1) were sampled every 2 to 3 days between July 5 and 20. Discrete water samples were analyzed for nitrate (NO_3) and ammonium (NH_4) (Barwell-Clarke & Whitney, 1996), and for dissolved organic nitrate (DON) (Solorzano & Sharp, 1980). Sea-water samples from S3 and S6 were filtered to determine concentrations of particulate organic carbon and nitrogen (POC/PON), using a CEC440 elemental analyzer. In addition to the water sampling program, a sediment trap moored near S3 at a depth of 50 m was sampled every 2 to 3 days to determine vertical transport of particulate nitrogen. Measurements show that of the available sources, NO_3 and DON together, in approximately equal proportions, account for 80–90% of biologically active nitrogen. Moreover, NO_3 and DON co-vary temporally; we thus use NO_3 concentration alone in the following discussion of the temporal variability of biogenic nitrogen at the three stations.

As seen in the gray-scale panels of Fig. 6, nitrate concentrations exhibit the same overall temporal pattern at all three stations, with quantitative differences related to the distance of each station from the mouth of the inlet. At all the stations, nitrate concentrations in the surface layer (0 to ~20 m) increase during spring tides (top panel). This increase is largest in magnitude and earliest in time at the sill station (S6), appearing at interior stations progressively later and with decreased magnitude. However, even at the southernmost interior station (S3), there is still distinct spring-tide enrichment of surface nitrate.

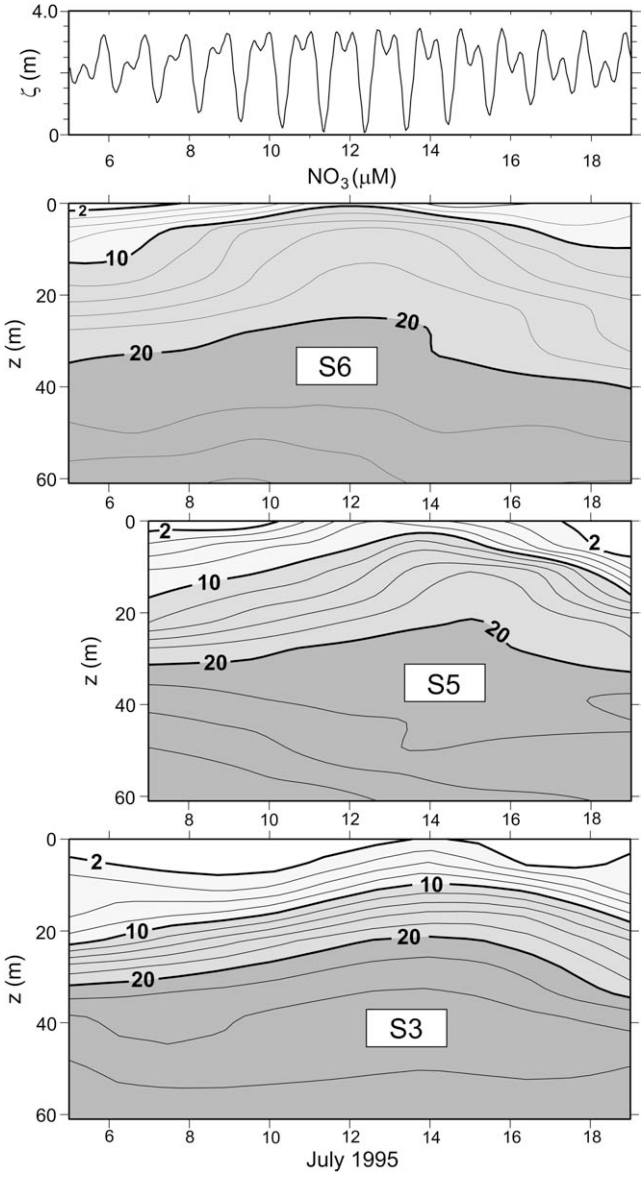

Fig. 6. Top panel: tidal height in Saanich Inlet, showing the strong neap/spring variation during the period of measurements. The gray-coded panels are time series of NO_3 concentration at three Saanich stations (see Fig. 1 for locations). Each station shows a pronounced neap/spring variation in near-surface NO_3.

Fig. 7 shows that the increase in surface-layer nitrogen at S3 is highly correlated with salinity, S (which is in turn highly anti-correlated with temperature, T, during the summer period of these measurements), as would be expected if the surface layer were advecting out of the inlet, and being replaced by upwelled deeper waters. The effect of this resupply of nitrate to the surface layer may be seen in the dramatic increases in both the concentration of suspended PON (Fig. 7b) and the rate of PON export, as measured at the 50 m sediment trap (Fig. 7c), that are observed at the end of the time series, several days past peak spring tides. Such a time lag between resupply of a limiting nutrient and increase in suspended particulates (phytoplankton) is to be expected, given finite times required for phytoplankton growth. Export production has a potentially slower time scale, associated with processing of the subsequent burst of primary production by the resident zooplankton. However, the rise in PON and that in export production are observed to occur nearly simultaneously, at least as well as can be determined from the time resolution of the water and trap-sampling sequence. Absence of a significant time lag between these two variables suggests that most export production is associated with rapidly sinking fecal pellets

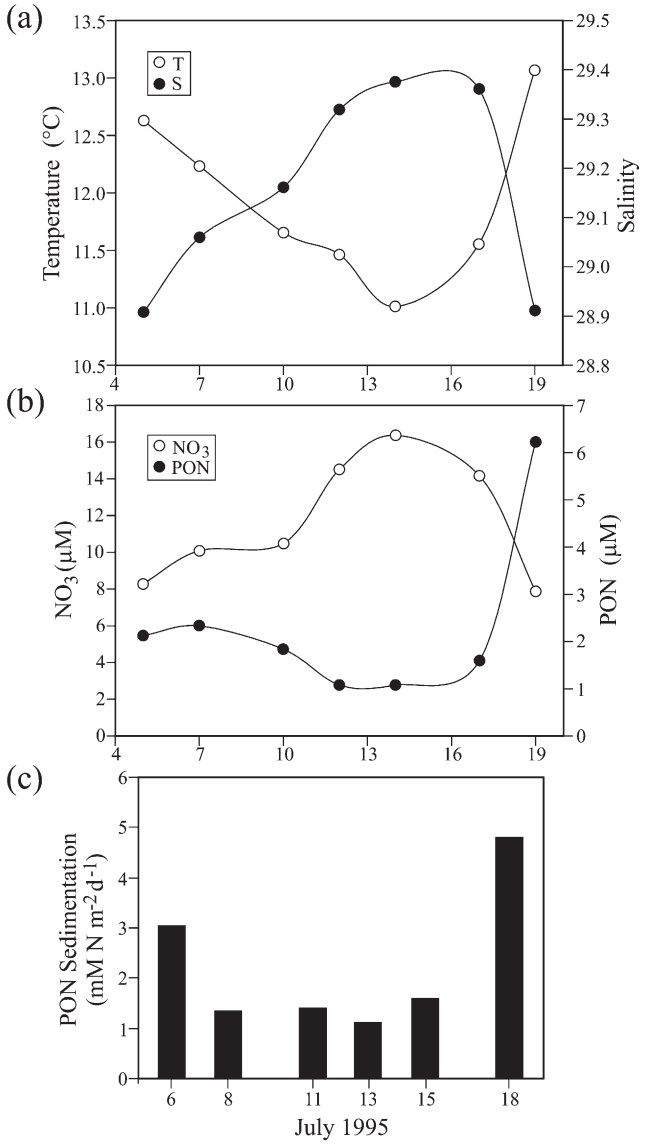

Fig. 7. Time series of (a) temperature, T, and salinity, S, (b) nitrate NO_3 and PON averaged over the upper 35 m of the water column from samples collected at 0, 5, 10, 15, 20, 30, and 40 m, and (c) sedimentation rate of PON measured by a sediment trap moored at 50 m depth. All measurements were made at Station S3.

produced by macro-zooplankton, a conclusion consistent with analyses of trap material collected in this study and in former studies on Saanich Inlet (Sancetta, 1989).

The previously mentioned interpretation assumes that the observed changes in particulate and export nitrogen are produced by local phytoplankton growth and subsequent zooplankton grazing, fueled by vertical resupply of NO_3, a limiting nutrient. However, because the time lag observed between the increase in NO_3 and subsequent increases in particulates happens to coincide roughly with the time interval between spring and neap tides, an alternate interpretation could be that the return to an inverse estuarine circulation characteristic of neap tides has advected increased particulates to the trap site from further north in the inlet. We think this advective explanation is unlikely, given the drifter evidence of weak recirculating flows during neap tides (Fig. 4a).

5. Box model of Saanich Inlet and environs

The observed changes in large-scale salinity distributions, reinforced by the surface drifter measurements, make it clear that there are large-scale movements of low-salinity surface waters out of the inlet and then back into it, during the course of a 2-week spring/neap tidal cycle. Observed changes in biogenic nitrogen suggest that these motions are associated with major impacts on the summertime biological productivity of Saanich Inlet. The fact that such impacts are observed at station S3, well away from the mouth of the inlet, indicates that the process that generates the horizontal motions must act over the entire inlet, not merely in frontal regions near its mouth. We suggest that pressure forces resulting from tidally forced changes of stratification outside the inlet are responsible for generating surface-layer outflow during spring tides. Recalling that the dominant source of summer freshwater is outside Saanich Inlet, surface-layer salinities outside the inlet fall below those inside the inlet (at the same depth) when tidal mixing is weak during neap tides. The resulting horizontal density (salinity) difference provides a pressure force that causes flow into the inlet in a surface layer and out of it at depth, i.e. the inverse estuarine circulation typical of Saanich Inlet. However, as tidal flows increase towards spring tides, strengthened vertical mixing outside the inlet erodes surface-layer salinities outside the inlet, but not within it. If enhanced tidal mixing causes vertical salinity fluxes that are sufficiently large compared with the continuing freshwater flux, surface-layer salinities outside the inlet may fall below those within it, reversing the pressure gradient and, hence, the flow directions. This pressure-gradient mechanism accounts for the major observational features described in the previous sections, namely the inlet-scale response and the association of flow reversals with spring-tide-induced changes in stratification *outside* the inlet.

A simple box model has been formulated to illustrate the interaction of stabilizing freshwater forcing and destabilizing tidal mixing in the operation of this mechanism. The model is roughly scaled to the dimensions of Saanich Inlet and used to predict periods of outflow, hence nutrient resupply, during the summer of 1975, for which the nutrient measurements of Takahashi et al. (1977) were taken. The box model, shown schematically in Fig. 8, consists of two 'basins', each represented by a thin upper layer, extending from the surface to 20 m, approximately the depth of the halocline within Saanich Inlet, and a lower layer of thickness, $h = 60$ m, extending from 20 to 80 m, an approximate depth of the channels outside its mouth (labeled generically 'Haro Strait').

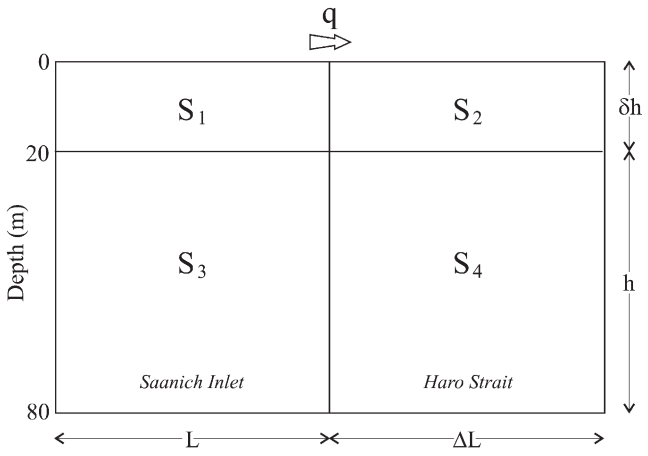

Fig. 8. Schematic of box model of Saanich Inlet and environs (for details see text and Appendix A).

The inlet is assumed to be 20 km long (L) and, on average, 2 km wide. The adjoining region represents neighboring areas, such as Satellite and Swanson Channels, as well as parts of Haro Strait itself. In the model results presented in this study, the effective area of this region is taken equal to that of Saanich, i.e. $\Delta = 1$.

Mass transport $q \equiv Q_o(\rho_2 - \rho_1)$ is assumed to vary with a pressure head associated with the difference in densities of the two upper boxes. This parameterization, due originally to Stommel (1961), has been widely used in studies of the thermohaline circulation (Whitehead, 1995), and has recently been applied to shallow inverse estuaries (Hearn, 1998). The transport q is defined as positive for outward surface-layer flow, as illustrated in Fig. 8. The horizontal flow between the surface boxes is assumed to be accommodated by up/downwelling across vertical box boundaries and return horizontal flow between the lower boxes. Thus, with surface-layer transport in the direction shown, water is advected into the deep box (3) of Saanich Inlet and upwelled into the surface box (1).

Density variations are assumed to be dominated by variations in salinity (although temperature (T) also influences density, atmospheric forcing of T is uniform over the limited horizontal scale of this model, so will not contribute to *differential* forcing of surface-layer densities). Since the model is focused on the summer phytoplankton growth season, (local) winter freshwater inputs are ignored, and the model is forced by equivalent salt fluxes associated with: (a) the annual freshet of the Fraser River, input to the upper box of the outer basin; and (b) a late-summer input of saline water to the lower outer box. The latter salt flux is associated with the annual appearance in Haro Strait of saline California Current waters that upwell onto the outer shelf of Vancouver Island in the summer and are entrained into the estuarine inflow that proceeds landward in the deep Strait of Juan de Fuca (Thomson, 1981). In the normalized forcing functions, shown in Fig. 9a, the amplitude of the saline inflow function is set equal to that of the freshwater function in order to preserve annually averaged mean salinity in the system (for details see Appendix A). However, temporal variation occurs within the annual cycle because of the time lag, τ, between the two processes. In the simulation shown, freshet starts at the end of May and peaks at the end of June; τ is taken to be 2 months. Further details of the full equations for conservation of salt in this box-model system, as well as the salt flux-forcing functions used to drive it, are presented in the Appendix A.

Finally, it is necessary to parameterize K_v, the vertical diffusivity of tidal mixing in the model. Between the two inside boxes, we set $K_v = 0$, consistent with previously discussed evidence for low turbulent diffusion within Saanich Inlet. Between the two outside boxes, we use the relation of Osborn (1980)

$$K_v \sim \frac{\varepsilon}{N^2} \tag{1}$$

relating turbulent kinetic energy dissipation rate, ε, and the buoyancy frequency $N = (-g\rho_o^{-1}\partial\rho/\partial z)^{1/2}$. Defining u_e as a characteristic speed and $t_e \sim u_e/l_e$ as a characteristic time scale for the large eddies (length scale l_e) of the turbulent field and substituting the standard scaling relation $\varepsilon \sim u_e^2/t_e$ (Tennekes & Lumley, 1972), Eq. (1) becomes

$$K_v \sim \frac{u_e^2}{N^2 t_e} \tag{2}$$

an expression that is closed by assuming that $u_e \propto U$, where U is a typical tidal speed, and that $t_e \propto N^{-1}$, i.e. the turbulent overturning time scale is set by the local buoyancy period. The latter assumption implies continual strong buoyancy control of turbulent motions, since it implies that a turbulent Froude number $Fr_e = u_e/Nl_e$ is always of O(1). An annual time series of $U(t)$ is determined by first-differencing observed tidal heights at a tidal station (Fulford Harbour) just off Satellite Channel. Then, using $N \sim (\Delta\rho)^{1/2}$, where $\Delta\rho = (\rho_4 - \rho_2)$ is the density difference between the surface and deep boxes in 'Haro Strait'

$$K_v \sim \frac{U^2}{N} \text{ or } K_v = K_o \frac{U^2}{(\Delta\rho)^{1/2}} \tag{3}$$

where K_o is a coefficient necessary to give magnitude (and the appropriate dimensions) to the scale relationship in Eq. (3). This expression for K_v involves system properties that are both external (U) and inherent ($\Delta\rho$), in the sense of evolving with evolution of model properties. Imposing such (computed) vertical diffusion at all the times was found to produce very smooth evolution of box salinity fields (not shown), unlike the on/off behavior suggested by the observations. We obtained more abruptly varying flows, consistent with the character of the observations, by adding an ad hoc threshold

criterion[1], requiring that the diffusivity given by Eq. (3) be imposed only when a critical Reynolds number Re_c is exceeded by a mean-flow Reynolds number $Re \equiv UH/v$ based on the typical barotropic tidal speed U used in Eq. (3) and the depth $H = h(1+\delta)$ corresponding to minimum water-column depth in the approach passages.

The adjustable parameters of the model are Q_o, the coefficient that sets the magnitude of flow resulting from a given pressure (density) difference, the magnitude F_o of the freshet-forcing function, the diffusion coefficient K_o, and a value for the critical Reynolds number Re_c. We first estimated F_o using an average value ($Q_r = 6000\ m^3\ s^{-1}$) of the Fraser River peak freshet flow, transformed to an equivalent salt flux through the relationship $F_o = Q_r S_o / V_o$ (Gill, 1982; see Appendix A). We then chose values for Q_o and K_o, which produced observationally reasonable summer salinities in the Saanich Inlet boxes for which we have the most observational information. Although a full discussion of parameter sensitivities of the box model is beyond the scope of this article, it should be noted that were the model forced with larger or smaller values of Fraser flow, results similar to those presented here can be achieved by adjustments to Q_o and/or K_o. Alternately, leaving the chosen parameters constant, while allowing F_o to vary over the range observed for peak Fraser River freshet flow, model results for the box salinities vary within observationally reasonable ranges. The final parameter, Re_c, has relatively little effect on the annual cycle of mean salinities, but more substantial effect on the *difference* $(S_2 - S_1)$ between the salinities of the upper layers, hence on the potential for periodic flow reversals. With $Re_c = 0$, which corresponds to K_v 'on' at all times, the flow is into the inlet at the surface from April until mid-August, when it reverses to a (winter) condition of surface outflow, i.e. flow direction reverses only once a year. Increasing Re_c gradually, we find that values of Re_c at around 0.5 produced occasional flow reversals during the summer season. As Re_c approaches 1 (corresponding to $K_v = 0$ at all times), the system approaches an uninteresting advective limit.

As an example of the behavior of this model, Fig. 9 shows results forced with the annual time series of the freshwater and deepwater-forcing functions shown, and values of $F_o = 5.3 \times 10^{-6}[S]\ s^{-1}$, $Q_o = 2 \times 10^{-3}\ m^3 s^{-1}$, $K_o = 1 \times 10^{-3}(m^{7/2}\ s^{-2}\ kg^{-1/2})$, $Re_c = 0.4$. To compare at least qualitatively with observations taken by Takahashi et al. (1977) in 1975, tidal heights observed during 1975 are used to determine U, as previously described. Fig. 9b shows the resultant time series of $Re/Re_c = U/U_c$: turbulent diffusion with K_v calculated from Eq. (3) is turned on only when $Re/Re_c > 1$ (i.e. above the horizontal line in Fig. 9b). The resultant annual cycle of salinities in the four boxes, calculated from an initial state in which both basins are weakly stratified, is seen in Fig. 9c. Fig. 9d shows the associated evolution of stratification, represented respectively in 'Haro Strait' and 'Saanich Inlet' by the vertical salinity differences $(S_4 - S_2)$ and $(S_3 - S_1)$, as well as the sense of advective flow $q = Q_o(\rho_2 - \rho_1) \propto (S_2 - S_1)$ forced by the horizontal density (salinity) difference between the two upper boxes.

Arrival of the Fraser River freshet is signaled first by a strong decline in the salinity (S_2) of the upper Haro box, quickly communicated to the upper Saanich box (S_1) by advection in the inverse-estuary sense. During this period of early June to late July, stability increases in both basins: however, there are brief intervals (shaded in Fig. 9d), coincident with spring tides, when tidal mixing in the Haro boxes is sufficiently strong that $S_2 > S_1$ and the advective flow temporarily reverses, i.e. the surface-layer flows *out* of Saanich Inlet. During late July and August, as the freshet wanes, but before the increase in stratification outside the inlet associated with arrival of the saline deepwater pulse, spring tides of similar or even lower magnitude lead to increasing periods of surface-layer outflows. With the arrival of the saline deepwater pulse, S_4 increases rapidly. As this salt is mixed upwards on successive spring tides, increasing the density of the surface 'Haro Strait' box, the outflow periods in which S_2 exceeds S_1 lengthen, and finally become continuous by the mid-winter (December) semi-annual maximum of the tides.

As seen in Fig. 9, this model predicts summer outflows, of increasing duration, associated with spring tides in late June/early July, early August and early September, roughly coincident with all but one of the sharp increases of nitrate observed during the summer measurements by Takahashi et al. (1977). Closer comparison of model predictions with measurements is not warranted, because deepwater renewal, one of the two major physical-forcing functions for the model, is poorly constrained by observations. While the timing of *potential* renewal events is set by the tidal velocities, which

[1] It is more usually assumed that the appropriate condition for initiation of turbulence in a stratified fluid is that of $Fr = 1$. However, a preliminary attempt to 'turn on' turbulent mixing with a constant (large) diffusivity only when a Froude number criterion was met led to a phenomenon labeled 'runaway stratification' by Simpson, Brown, Matthews, and Allen (1990). After an initial period during which the stratification varied (a period whose length depends upon the initial imposed stratification), the system eventually achieved a degree of stratification which, given finite tidal velocities and a constant diffusivity, could no longer be reduced sufficiently to trigger turbulent mixing. After this point, the stratification increased monotonically, rapidly reaching totally unrealistic values. In contrast, our parameterization implies that a sufficiently high Re will initiate turbulence regardless of the stratification. Once initiated, however, the resulting turbulence is strongly influenced by the stratification, through the requirement that the turbulent Froude number Fr is always of O(1). We offer no justification for this very different parameterization beyond the obvious—it works (in the sense of providing stable model solutions), while parameterization based on Fr does not.

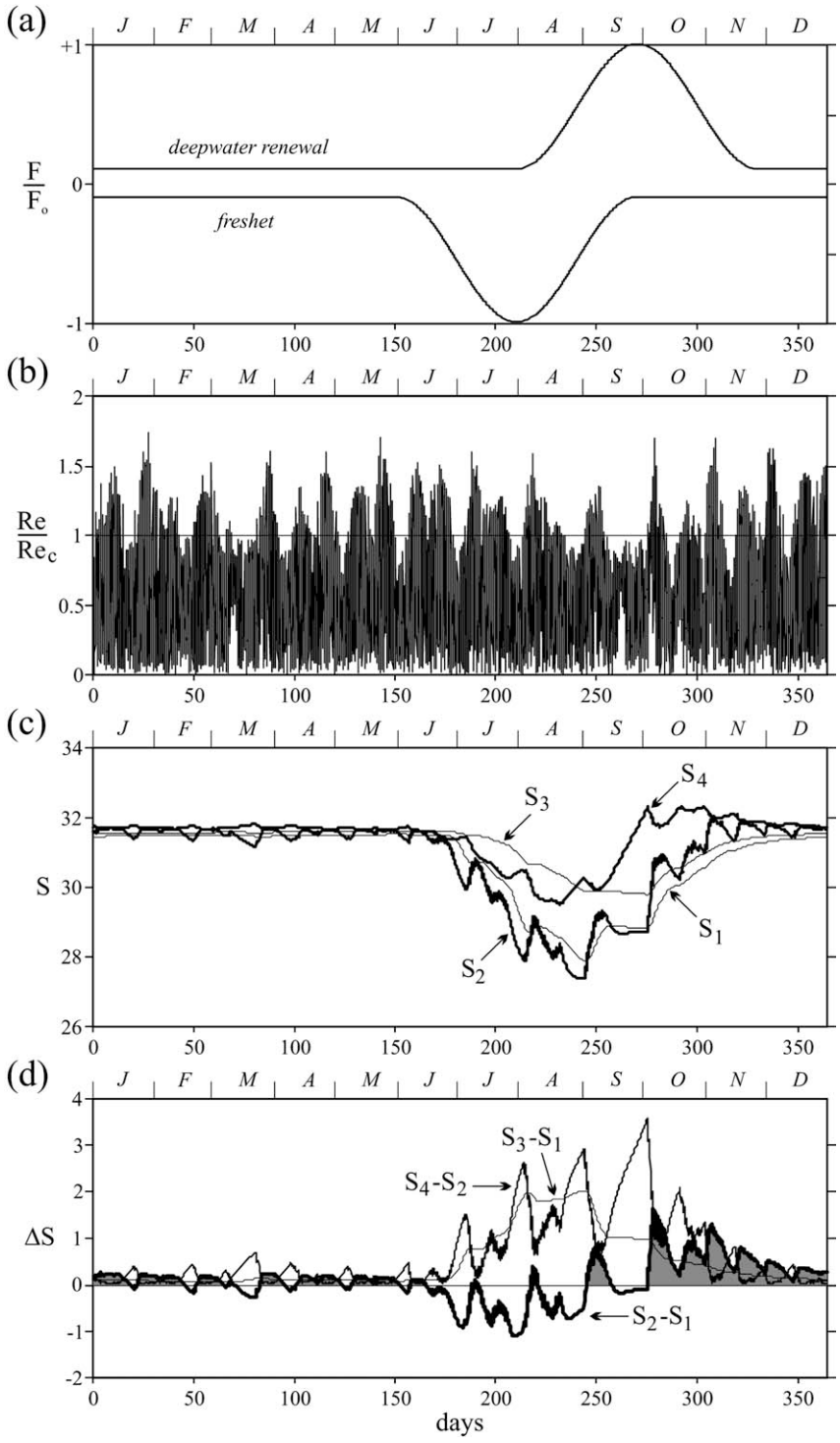

Fig. 9. (a) Equivalent salt-forcing functions (F) normalized by F_o, an amplitude derived from Fraser River freshet peak flow: freshwater input appears as negative salt forcing. (b) The function Re/Re_c used to turn 'Haro Strait' mixing on/off (for details see text). (c) Predicted annual cycles of salinities in the four model boxes. (d) Predicted annual cycle of density stratification inside and outside Saanich Inlet, represented respectively by salinity differences (S_3-S_1) and (S_4-S_2). Surface-layer flow is out of Saanich Inlet when $(S_2-S_1) > 0$.

vary relatively little from year to year, the occurrence and/or duration of *actual* renewal events during a particular year depends upon magnitude and timing of both the Fraser freshet and the deepwater renewal event. While characteristics of the Fraser freshet are well determined by river-flow monitoring dating back to 1912, there are no corresponding records of timing or magnitude of the dense deepwater inflows. All that is known

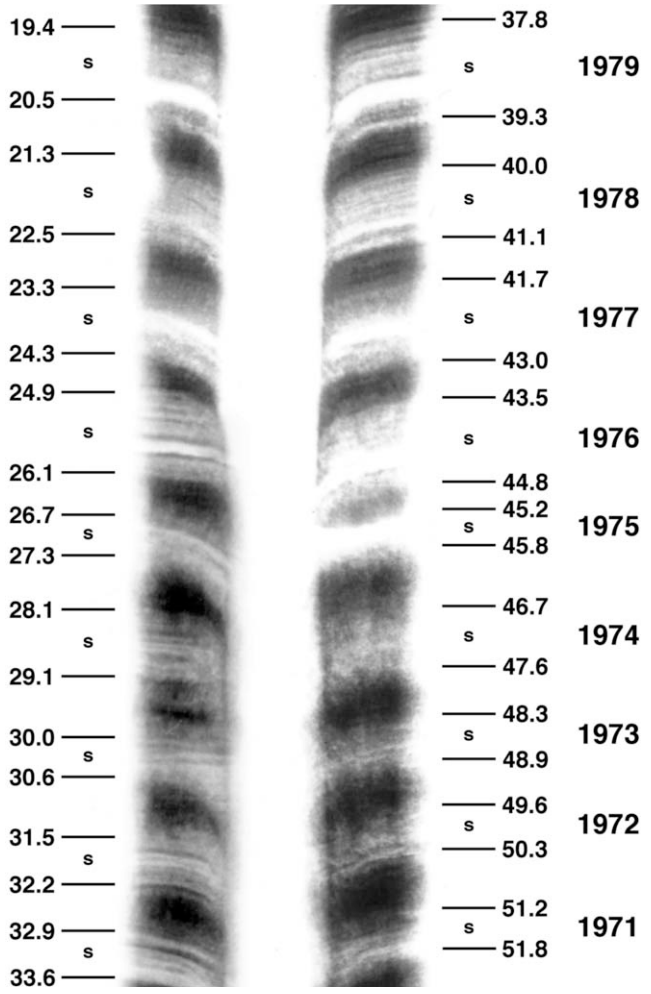

Fig. 10. X-radiographs over several of the annual varves seen in replicate freeze-cores taken at a Saanich Inlet site roughly midway between Stations S4 and S5 (Fig. 1). Very thin micro-varves can be distinguished within most of the light (summer) bands: these may result from quasi-periodic 'mini-blooms' resupplied with nutrients via the physical processes described in this article. (Core radiographs courtesy of V. Tunnicliffe, University of Victoria.)

about these inflows is that they generally occur in late summer or early fall, and must, on average, balance the net summer annual freshwater inputs, since the mean salinity of Saanich Inlet has not been observed to change during the extent of historical measurements. Further work, in progress, will attempt to determine which features of the physical-forcing functions produce the most variation in timing and duration of the sporadic summer nutrient renewal events that make a major contribution to the summer productivity of this inlet.

6. A sedimentary record of summer mini-blooms?

The anoxic bottom waters of Saanich Inlet prevent the usual macro-fauna from colonizing its sediments, which thus remain undisturbed by burrowing and digging animals. Gross, Gucluer, Creager, and Dawson (1963) described the resulting seasonal strata preserved in these sediments, seen as a regular sequence of dark and light bands (varves) in sediment cores. An annual cycle consists of one light and one dark band, resulting, respectively, from the deposition of biogenic material (light) produced during the growing period in summer season and of terrigenous material (dark) washed into the inlet by winter runoff. Gross et al. (1963) also remarked that the light-colored biogenic (summer) laminae commonly contained even finer layers. Fig. 10 contains examples of such micro-varves, seen in multi-year segments of modern freeze-cores, while other examples may be found in McQuoid and Hobson (1997) and Dean, Kemp, and Pearce (2001). Viewed as individual light layers superimposed upon a dark background, this fine detail within the productive summer season could be sedimentary evidence of summer 'mini-blooms' produced by semi-periodic nutrient resupply by the tidally forced renewal process discussed in this article. Viewed alternately as individual dark layers superimposed upon a light background, the micro-varves might equally well be an evidence of the effects of intense local run-off events superimposed upon biological production that is relatively constant throughout the summer growing season. The latter interpretation seems much less likely, both because of the existing observational evidence of episodic biological production, and because Saanich Inlet lies within a region with normally dry summers (Herlinveaux, 1962). However, future work will attempt to differentiate between these two possibilities by examining historical records of both Fraser-River flow and local rainfall in relation to the sedimentary record of micro-varves.

7. Discussion and conclusions

We feel confident that the observations and model presented in this study provide a major part of the explanation for the high primary production known to characterize Saanich Inlet. Enhanced primary productivity results from a combination of effects. First, the sheltered nature of the inlet with respect to summer-time winds and tidal mixing leads to a stably stratified environment in which phytoplankton are retained in a shallow, well-lighted surface layer. Next, surface-layer macro-nutrients depleted by phytoplankton blooms triggered by these favorable light conditions are resupplied on a semi-regular basis throughout the growing season. The resupply mechanism is inlet-scale upwelling, driven by pressure-gradient forces set up by effects of strong spring-tidal mixing on vertical density gradients outside the inlet. Legendre (1981) argued that regions of especially high primary productivity must be characterized by a temporal sequence of locally intense mixing

followed by stable stratification. In Saanich Inlet, the separation between favorable nutrient and light conditions is spatial rather than temporal in nature, with advection an essential connecting element. Finally, we note that in the high-growth periods between nutrient renewal events, weak inverse estuarine circulation will retain local primary production within Saanich Inlet, as well as import material from the frontal region at its mouth (Hobson and McQuoid, 2001; Parsons et al., 1983). Coupled with high primary productivity, this retention mechanism also contributes to the high levels of secondary and export productions, which are observed in Saanich Inlet.

The present study of Saanich Inlet documents a system in which nutrients necessary for biological production are supplied to the euphotic zone of a highly productive region through processes that act *outside the region itself*. The process by which intense, but highly localized, mixing affects the phytoplankton production over large spatial scales through horizontal redistribution in an estuarine circulation is not unique to Saanich Inlet. Although not concerned with biological consequences, Stacey and Gratton (2001) have recently modeled 'reverse renewal' in the two-silled fjord of the Saguenay, off the St. Lawrence estuary, as a result of pressure gradients associated with more vigorous M_2 tidal mixing in the outer basin than the inner basin. In another example, Crawford (1991) estimated that the dominant supply of nutrients to the highly productive ecosystem on the southern British Columbia shelf is through advection in the surface layer that exits the Strait of Juan de Fuca at the south end of Vancouver Island (Fig. 1). Nutrients are mixed into this layer predominantly within the inter-island passes and channels at the southeast end of the Strait of Georgia, far from the outer shelf region where they are utilized. We suggest that the 'action-at-a-distance' mechanism of nutrient resupply to phytoplankton populations that we have documented in Saanich Inlet is probably typical of estuarine and coastal regions of strong freshwater influence.

Finally, we warn that marine ecosystems in estuarine areas that are strongly influenced by turbulent mixing can be severely impacted by potential effects of global warming (increased surface temperatures, increased or decreased precipitation/run-off) on the stratification of the environment in which they are embedded.

Acknowledgements

Support for the observational part of this study was provided by the BC Ministry of Environment, as part of the SIS, and by Fisheries and Oceans Canada. D.S. and F.W. would like to thank the large numbers of volunteers, staff, and visiting scientists, whose efforts were essential for the success of the observational effort in Saanich Inlet during the summer of 1995.

Appendix A

The four-box model configuration is shown in Fig. 8. For Box j, we denote thickness as h_j and area as A_j. Box salinity (salt/unit mass) is given by S_j and the mass of water in the jth box is $m_j = \rho_o V_j = \rho_o h_j A_j$, where ρ_o is a reference density. Equations for the time rate of change of the mass of salt $m_j S_j$ in the jth box are given by

$$m_1 \frac{dS_1}{dt} = q_o^+(S_3 - S_1) + q_o^-(S_2 - S_1) + \rho_o w_i A_i (S_3 - S_1) \quad \text{(A1)}$$

$$m_2 \frac{dS_2}{dt} = q_o^+(S_1 - S_2) + q_o^-(S_4 - S_2) + \rho_o w_o A_o (S_4 - S_2) - m_2 F S_2 \quad \text{(A2)}$$

$$m_3 \frac{dS_3}{dt} = q_o^+(S_4 - S_2) + q_o^-(S_1 - S_3) - \rho_o w_i A_i (S_3 - S_1) \quad \text{(A3)}$$

$$m_4 \frac{dS_4}{dt} = q_o^+(S_2 - S_4) + q_o^-(S_3 - S_4) + \rho_o w_o A_o (S_4 - S_2) + m_4 F S_4 \quad \text{(A4)}$$

Advection between boxes is characterized by a flux of mass $q_o = Q_o(\rho_2 - \rho_1)$ proportional to the density difference between the two upper layers (Stommel, 1961). To allow for reversal of the flow direction with reversal in sign of this difference, we use the definitions of Thual and McWilliams (1992)

$$q_o^+ = \frac{1}{2}(|\, q_o \,| + q_o) \quad \text{(A4)}$$

$$q_o^- = \frac{1}{2}(|\, q_o \,| - q_o) \quad \text{(A4)}$$

which automatically select the appropriate upstream differencing. Turbulent vertical diffusion is represented by entrainment velocities, respectively w_i and w_o inside (i) and outside (o) Saanich Inlet, and acting across the respective interfacial areas $A_i = A_1 = A_3$ and $A_o = A_2 = A_4$. FS_2 and FS_4, with units of salt per unit mass (salinity) per unit time, represent external-forcing of the system through addition of freshwater and saltwater, respectively, to boxes 2 and 4.

Dividing Eqs. (A1)–(A4) by m_1 and defining $\delta \equiv h/H = h_1/h_3 = h_2/h_4$ and $\Delta \equiv A_2/A_1$, the equations can be rewritten as:

$$\frac{dS_1}{dt} = q^+(S_3 - S_1) + q^-(S_2 - S_1) + W_i(S_3 - S_1) \quad \text{(A5)}$$

$$\frac{dS_2}{dt} = \frac{1}{\Delta}(q^+(S_1 - S_2) + q^-(S_4 - S_2)) + W_o(S_4 - S_2) - F S_2 \quad \text{(A6)}$$

$$\frac{dS_3}{dt} = \delta(q^+(S_4 - S_3) + q^-(S_1 - S_3) - W_i(S_3 - S_1)) \tag{A7}$$

$$\frac{dS_4}{dt} = \frac{\delta}{\Delta}(q^+(S_2 - S_4) + q^-(S_3 - S_4)) - \delta W_o(S_4 - S_2) + FS_4 \tag{A8}$$

in which $W_{i/o} \equiv w_{i/o}/h$ and $q^{+/-} \equiv q_o^{+/-}/m_1$ have units of inverse time. Over an annual cycle, conservation of the total mass of salt in the system requires that

$$\frac{d}{dt}\left(\sum_{j=1}^{4} m_j S_j\right) = 0$$

hence that $\int(m_4 FS_4 - m_2 FS_2) = 0$, where the integral is over 1 year.

In keeping with the exploratory nature of the box model, we use a very simple functional form for the required (salinity) forcing function(s). Freshet is represented by a rectified cosine of temporal extent T_w, peaking at T_p, superimposed upon a much smaller, constant background 'winter' level. The associated rate of change of salinity (in units of $[S]\,s^{-1}$) is

$$FS_2(t) = F(t) = F_o\left(0.1 - 0.45\left(1 - \cos\left(\frac{2\pi(t - T_p)}{T_w}\right)\right)\right)$$

Peak magnitude F_o was estimated by converting average peak Fraser River flow of $Q_F = 6000\ m^3 s^{-1}$ to equivalent salt forcing under the assumptions of Gill (1982): thus $F_o = Q_r S_o / V_o = 5.3 \times 10^{-6}\ [S]\ s^{-1}$, where $V_o = 4 \times 10^{10}\ m^3$ is an estimate of the volume of the upper Strait of Georgia into which the Fraser River freshwater is distributed and $S_o = 35$ is an average salinity of the Strait. The required salt conservation is then simply enforced by setting $FS_4(t) = \delta F(t + \tau)$, where τ is a time offset. Fig. 9a shows normalized forcing functions F/F_o (plotting freshet as negative) for $T_p =$ Year day 181, $T_w = 60$ days and $\tau = 60$ days.

References

Anderson, J. S., & Devol, A. H. (1973). Deep-water renewal in Saanich Inlet, an intermittently anoxic basin. *Estuarine, Coastal and Marine Science 1*, 1–10.

Barwell-Clarke, J., & Whitney, F. (1996). Institute of Ocean Sciences nutrient methods and analysis. *Canadian technical report on hydrography and ocean science 182* (63 pp.). Institute of Ocean Sciences, Sidney, BC.

Crawford, W. R. (1991). Tidal mixing and nutrient flux in the waters of southwest British Columbia. In B. Bruce, & J. Parker (Eds.), *Tidal hydrodynamics* (pp. 855–869). New York: Wiley.

Dean, J. M., Kemp, A. E. S., & Pearce, R. B. (2001). Palaeo-flux records from electron microscope studies of Holocene laminated sediments, Saanich Inlet, British Columbia. *Marine Geology 174*, 139–158.

Farmer, D. M., D'Asaro, E. A., Trevorrow, M. V., & Dairiki, G. T. (1994). Three-dimensional structure in a tidal convergence front. *Continental Shelf Research 15*(13), 1649–1673.

Farmer, D. M., & Freeland, H. J. (1983). The physical oceanography of fjords. *Progress in Oceanography 12*(2), 147–219.

Gargett, A. E. (1994). Observing turbulence with a modified acoustic Doppler current profiler. *Journal of Atmospheric and Oceanic Technology 116*, 1592–1610.

Gargett, A. E. (1997). 'Theories' and techniques for observing turbulence in the ocean euphotic zone. In C. Marrasé, E. Saiz, & J. M. Redondo (Eds.), Lecture notes on plankton and turbulence. *Scientia Marina* 61(Suppl.), 25–45.

Gargett, A. E. (1999). Velcro measurement of turbulence kinetic energy dissipation rate ε. *Journal of Atmospheric and Oceanic Technology 16*(12), 1973–1993.

Gill, A. E. (1982). Atmosphere–ocean dynamics. *International geophysics series 30* (662 pp.). New York, Academic Press.

Griffin, D. A., & LeBlond, P. H. (1990). Estuary/ocean exchange controlled by spring–neap tidal mixing. *Estuarine, Coastal and Shelf Science 30*, 275–297.

Gross, M. G., Gucluer, S. M., Creager, J. S., & Dawson, W. A. (1963). Varved marine sediments in a stagnant fjord. *Science 141*, 918–919.

Hearn, C. J. (1998). Application of the Stommel model to shallow Mediterranean estuaries and their characterization. *Journal of Geophysics Research 103*(C5), 10391–10404.

Herlinveaux, R. H. (1962). Oceanography of Saanich Inlet in Vancouver Island, British Columbia. *Journal of Fishery Research Board Canada 19*(1), 1–37.

Hobson, L., & McQuoid, M. R. (2001). Pelagic diatom assemblages are good indicators of mixed water intrusion into Saanich Inlet, a stratified fjord in Vancouver Island. *Marine Geology 174*, 125–138.

Legendre, L. (1981). Hydrodynamic control of marine phytoplankton production: the paradox of stability. In J. Nihoul (Ed.), *Eco-hydrodynamics. Proceedings of the 12th international Liege colloquium on ocean hydrodynamics*.

Lu, Y., & Lueck, R. G. (1999). Using a broad-band ADCP in a tidal channel. Part II. Turbulence. *Journal of Atmospheric and Oceanic Technology 16*(11), 1568–1579.

McQuoid, M. R., & Hobson, L. A. (1997). A 91-year record of seasonal and interannual variability of diatoms from laminated sediments in Saanich Inlet, British Columbia. *Journal of Plankton Research* 19(1), 173–194.

Osborn, T. R. (1980). Estimates of the local rate of vertical diffusion from dissipation measurements. *Journal of Physical Oceanography 10*, 83–89.

Parsons, T. R., Perry, R. I., Nutbrown, E. D., Hsieh, W., & Lalli, C. M. (1983). Frontal zone analysis at the mouth of Saanich Inlet, British Columbia, Canada. *Marine Biology 73*, 1–5.

Sancetta, C. (1989). Spatial and temporal trends of diatom flux in British Columbian fjords. *Journal of Plankton Research 11*(3), 503–520.

Simpson, J. H., Brown, J., Matthews, J. P., & Allen, G. (1990). Tidal straining, density currents and stirring in the control of estuarine stratification. *Estuaries 13*(2), 125–132.

Solorzano, L., & Sharp, J. H. (1980). Determination of total dissolved nitrogen in natural waters. *Limnology and Oceanography 25*, 751–754.

Stacey, M. W., & Gratton, Y. (2001). The energetics and tidally induced reverse renewal in a two-silled fjord. *Journal of Physical Oceanography 31*, 1599–1615.

Stommel, H. (1961). Thermohaline convection with two stable regimes of flow. *Tellus 13*, 224–230.

Takahashi, M., Seibert, D. L., & Thomas, W. H. (1977). Occasional blooms of phytoplankton during summer in Saanich Inlet, BC, Canada. *Deep-Sea Research 24*, 775–780.

Tennekes, H., & Lumley, J. L. (1972). *A first course in turbulence*. (300 pp.). Cambridge: MIT Press.

Thomson, R. E. (1981). Oceanography of the British Columbia Coast. *Canadian special publication of fisheries and aquatic sciences no. 56* (291 pp.).

Thual, O., & McWilliams, J. C. (1992). The catastrophe structure of thermohaline convection in a two-dimensional fluid model and a comparison with low-order box models. *Geophysics Astrophysics and Fluid Dynamics 64*, 67–95.

Timothy, D. A., & Soon, M. Y. S. (2001). Primary production and deep-water oxygen content of two British Columbia fjords. *Marine Chemistry 73*, 37–51.

Whitehead, J. A. Jr. (1995). Thermohaline ocean processes and models. *Annual Review of Fluid Mechanics 27*, 89–113.